The role of charge and recombination-enhanced-defect-reaction effects in the dissociation of FeB pairs in p-type silicon under injection

Chang Sun[1,a)], Yan Zhu[2], Mattias Juhl[2], Wenjie Yang[1], Fiacre Rougieux[2], Ziv Hameiri[2] and Daniel Macdonald[1]

[1]Research School of Electrical, Energy & Materials Engineering, the Australian National University, Canberra, ACT 2601, Australia
[2]School of Photovoltaic and Renewable Energy Engineering, University of New South Wales, Sydney, NSW 2052, Australia

Abstract The dissociation of FeB pairs in p-type silicon under injection is often explained by the charge state change of interstitial Fe (Fe_i) from positive to neutral. It is also sometimes interpreted as a Recombination-Enhanced Defect Reaction (REDR) mechanism. The charge effect and the REDR have fundamentally different impacts on the dissociation/association reactions: the former changes the concentration of Fe_i^+, yet the latter changes the reaction rate constants. In this study, we have investigated and compared the two effects through measuring and analyzing the dynamics of the reactions. The results confirm that the dissociation of FeB under carrier injection cannot be purely attributed to the change of charge states. The extracted dissociation/association rate constant ratio shows an approximately linear dependence on the recombination rate on each FeB pair, indicating the REDR effect. The results allowed the two effects to be directly compared, highlighting the dominant role of the REDR effect in dissociating the pairs.

Fe is one of the main metallic impurities in photovoltaic silicon materials.[1,2] In B-doped p-type silicon (p-Si), the mobile, positively charged interstitial Fe (Fe_i^+) can be captured by the negatively charged B^-, forming FeB pairs at room temperature or slightly elevated temperatures.[1] FeB pairs can be dissociated at higher temperatures or under injection of excess carriers.[3] The temperature range from where the equilibrium is shifted from the associated state to the dissociated state depends on the B concentration [B].[4] The reversible dissociation and association reactions can be described as follows[3,5]

[a)] Corresponding author. E-mail: chang.sun@anu.edu.au.

This article has been accepted for publication and undergone full peer review but has not been through the copyediting, typesetting, pagination and proofreading process, which may lead to differences between this version and the Version of Record. Please cite this article as doi: 10.1002/pssr.202000520.

$$\mathrm{FeB} \underset{k_a}{\overset{k_d}{\rightleftharpoons}} \mathrm{Fe_i^+} + \mathrm{B^-}, \qquad (1)$$

with the *rate constants* k_d and k_a, respectively. The dissociation and association reactions have been investigated in numerous studies,[5-16] mostly within the framework of chemical interactions in silicon developed by Reiss *et al*. for Li-B pairing.[17]

In p-Si with [B]>1×10^{15} cm^{-3}, almost all Fe_i atoms are positively charged at room temperature in the dark. A substantial fraction of isolated (unpaired) Fe_i becomes neutral at elevated temperatures or under injection.[18] It is widely-agreed that reactions between metallic donors and dopant acceptors, such as Reaction (1), only occur when Coulomb attraction is present.[1,2] The dissociation of FeB pairs in p-Si under injection is often explained by the charge state change of Fe_i from positive to neutral.[1,13,19] However, the charge state of isolated Fe_i has not always been appropriately considered in previous studies. One example is that all isolated Fe_i atoms have been occasionally considered as reactants in Reaction (1) regardless of the charge state, which is potentially problematic when carrier injection or elevated temperatures are involved in the experiments.[7,8,11,15] Another example is the charge state prediction based on the electron quasi-Fermi level approximation under injection.[1,13,19] This leads to erroneous results for the Fe_i level in most circumstances as shown in Ref. [18]. Ref. [18] has proposed a rigorous model for the charge state of deep levels in silicon based on the Shockley-Read-Hall (SRH) statistics.

The dissociation of FeB under injection is sometimes referred to as a Recombination-Enhanced Defect Reaction (REDR).[6,13,20] As explained in Refs.[6,21], the local vibrational energy released from a recombination event at the defect center can promote defect reactions such as dissociation and diffusion. In theory, in the Arrhenius equation that determines the enhanced reaction rate constant, the pre-exponential factor and the activation energy will both differ from the equilibrium values, and the pre-exponential factor (the attempt frequency) will be proportional to the recombination rate.[6,13,20-22] Although the charge effect and the REDR are closely related,[20] each

effect has independent and distinct manifestations on Reaction (1):[21] the charge effect reduces [Fe_i^+] and thus the reverse reaction rate; yet the REDR effect is on the reaction rate constant k_d, and possibly k_a.[13] In spite of this fundamental difference, an experimental study that explicitly discusses, or distinguishes between their effects on Reaction (1) has not been reported.

In principle, the most straightforward way to determine the reaction rates of (1) is through a kinetics study. However, this approach has an inherent drawback under carrier injection, as [FeB] decreases and [Fe_i] (isolated) increases during the dissociation.[15] Consequently, both the lifetime and injection level will change over time when the illumination intensity is fixed. This results in changes in the recombination rate on the FeB pairs, as well as the charge state of isolated Fe_i. The reaction rates will therefore not be constant under these conditions, making the analysis complicated and unreliable. In contrast, the analysis of the dynamics (steady state)[8] can potentially provide more unambiguous information on the reaction rates. Such analysis is based on the fact that a lower illumination intensity dissociates FeB pairs less completely, resulting in a steady-state balance between dissociation and association, where FeB pairs and isolated Fe_i coexist.[8]

In this study, we aim to gain a deeper understanding of the roles that the charge effect and REDR effect play in the FeB dissociation under injection. The two effects will be more distinctly separated in comparison with previous reports. They will be investigated by measuring and analyzing the dynamics of Reaction (1) and its dependence on the illumination intensity.

Float-zone (FZ) B-doped silicon wafers with four doping levels [B]= 2.9×10^{16} cm^{-3}, 1.6×10^{16} cm^{-3}, 5.5×10^{15} cm^{-3}, and 1.4×10^{15} cm^{-3}, were included in this study. The doping levels were determined by eddy current-based dark conductance measurement. For each doping level, one to three samples were implanted with 70 keV Fe^{56} ions using different doses to result in volume Fe concentrations [Fe_i] in the 5.6×10^{11} cm^{-3} to 1×10^{13} cm^{-3} range (these are expected values from the implantation doses). The wafers were chemically etched and cleaned before the implantation. After implantation, the samples were cleaned again and annealed in a clean quartz tube furnace at 1000 °C in dry O_2 for

45 min, and in N_2 for 30 min, followed by cooling down to 700 °C with a cooling rate of 10 °C/s and then to room temperature in air. This annealing process allowed the implanted Fe atoms to achieve a uniform distribution throughout the thickness of the wafers, and to be quenched in the interstitial state, as well as growing a 60-nm-thick SiO_2 passivation film on each surface. The samples were then annealed in forming gas at 425 °C for 30 min to further improve the SiO_2 passivation.

The illumination-dependent steady-state fractions of FeB pairs and isolated Fe_i were determined based on lifetime measurements.[8,23] The injection-dependent lifetime measurements were conducted at room temperature, applying the Quasi-Steady-State Photo-Conductance (QSSPC) technique,[24] built in to a LIS-R1 PL imaging system from BT Imaging.[25] This system allows the adjustment of the peak laser intensity, I_{laser}, during the measurement. Every sample went through the following measurement sequence:

a) The fully-associated state was achieved by keeping the sample at room temperature in the dark for long enough, with the time length depending on the doping level.[9] The lifetime at the fully-associated state, τ_a, was then measured, using the lowest laser intensity (0.03 suns or lower) that minimized carrier injection while maintaining a good photo-conductance (PC) signal.

b) The sample was then exposed to an illumination intensity I_{lamp} on a temperature-controlled stage at 23±2 °C until a steady state was achieved. The illumination was provided by a halogen lamp and measured by a reference cell.[26] Repeated measurements were performed to ensure that a steady state was achieved. The lifetime at the steady state, τ_{ss}, was measured. During the measurement, I_{laser} was adjusted to a value around 1.3 I_{lamp}. The reason for this will be discussed later.

c) The sample was then exposed to a higher illumination intensity to achieve a new steady state before another lifetime measurement was conducted. This was repeated for several gradually increasing illumination intensities before a saturation effect became evident.

d) The fully-dissociated state was achieved by illuminating the sample with >10 suns for >5 min, on the temperature-controlled stage which kept the sample temperature <40 °C. Higher illumination intensities were used to ensure the achievement of the fully-dissociated state. The lifetime at the fully-dissociated state, τ_d, was measured at room temperature."

For the sample with [B]=2.9×10^{16} cm^{-3}, an additional set of measurements was conducted in the reverse direction: starting from the fully-dissociated state, steady-state lifetime measurement was repeated for the same, but gradually decreasing illumination intensities.

It was observed that for some of the samples, the PC signal was too noisy to generate reliable lifetime data, probably due to the non-ideal passivation quality of the SiO_2 films. The noisy data were not included in the analysis. For all of the samples, the SiO_2 films were removed using dilute HF solution, followed by a deposition of a 20-nm-thick AlO_x film on each side, using plasma-assisted ALD with a Beneq TFS200 reactor. The deposition temperature was approximately 175 °C. The coated samples were annealed in forming gas at 425 °C for 20 min to activate the surface passivation. It was found previously that the deposition or the activation of the AlO_x films does not affect [Fe_i] significantly.[27] The measurements described above were then conducted again. The AlO_x passivation allowed reliable lifetime data to be obtained from all the samples.

Some examples of the measured lifetime data are given in Figure 1: the fully-associated and fully-dissociated states, and two steady states achieved under 0.05 suns and 0.12 suns, are shown. The dashed lines show the linear relation between the lifetime and injection under fixed generation rates. Each dashed line crosses the corresponding lifetime data at the injection level achieved at the steady state, Δn_{ss}. I_{laser} was set a little higher than the lamp illumination intensity I_{lamp}, as previously mentioned, in order to make the highest measured injection level $\Delta n_{maxmeasured}$ (determined by I_{laser}) slightly exceed Δn_{ss} (determined by I_{lamp}). This ensured that Δn_{ss} is within the measured injection range, and thus can be conveniently estimated. Nevertheless, I_{laser} was set as close as possible to I_{lamp}, to minimize extra pairs dissociated by the laser.

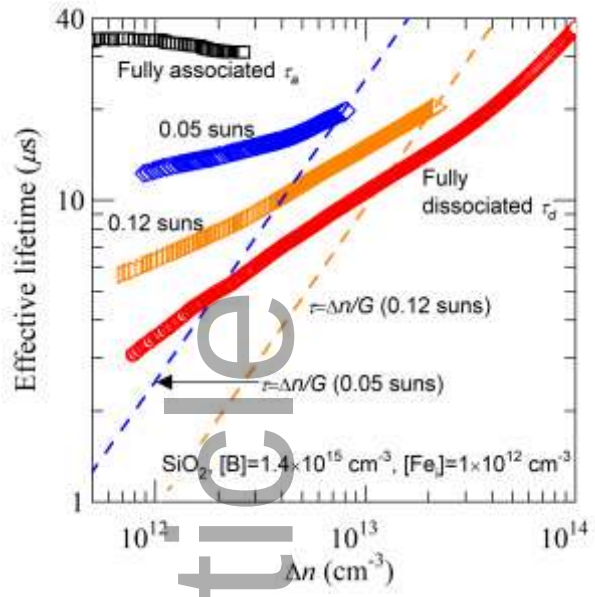

Figure 1. Injection-dependent lifetimes at the fully-associated state and the fully-dissociated state, and the steady-states achieved under 0.05 and 0.12 suns of a SiO_2-coated sample. For the latter two cases, the dashed lines show the linear relation between the lifetime and the injection level under the corresponding generation rates. The crossover point of the dashed line and the lifetime data indicates the injection level at the steady state.

The observed changes in lifetime are not likely to be caused by the light and elevated temperature-induced degradation (LeTID),[28,29] because: (1) none of the samples in this work was fired, whilst to create LeTID, a sample needs to be fired at >700 °C;[30] (2) the degradation of the low-injection lifetime is completely reversible after leaving the samples at room temperature for long enough, which is not an expected behaviour of LeTID; (3) the lifetime curves in Figure 1 indicate a crossover point at the injection level of 10^{14} cm^{-3}, which is a characteristic "fingerprint" of Fe_i in B-doped p-Si;[23,31] in contrast, lifetime degradation over the whole injection range is usually observed during the activation of LeTID.[29]

The dissociated fraction, i.e. the fraction of isolated Fe_i to the total [Fe_i], f_{iso}, can be calculated using τ_{ss}, τ_a, and τ_d:

$$1 - f_{iso} = \frac{\frac{1}{\tau_d} - \frac{1}{\tau_{ss}}}{\frac{1}{\tau_d} - \frac{1}{\tau_a}}. \qquad (2)$$

Similar to the method to determine [Fe_i] in B-doped p-Si,[23] the calculation is theoretically not affected by other recombination channels which are stable under illumination. The calculation does

not require defect parameters of Fe_i or FeB. Data within an injection range were used in the calculation, giving an average f_{iso} as well as an uncertainty range. The available injection range for the calculation is usually limited by τ_a, as it has the lowest $\Delta n_{maxmeasured}$. To make the best of the data, an already calculated fraction f_{iso1} (with lifetime τ_{ss1}) was often utilized to determine a new fraction f_{iso2} (with lifetime τ_{ss2}), via:

$$\frac{1-f_{iso2}}{1-f_{iso1}} = \frac{\frac{1}{\tau_d}-\frac{1}{\tau_{ss2}}}{\frac{1}{\tau_d}-\frac{1}{\tau_{ss1}}}. \qquad (3)$$

Taking the data in Figure 1 for example, after calculating the fraction at the 0.05 suns steady state using τ_a and τ_d, the 0.05 suns lifetime data instead of τ_a was used to calculate the fraction under 0.12 suns. This increased the upper limit of the available injection range from 2.6×10^{12} cm^{-3} to 8.1×10^{12} cm^{-3}.

The dissociated fraction data are shown in Figure 2 as a function of Δn_{ss}. It is evident that for the sample with [B]= 2.9×10^{16} cm^{-3} in Figure 2(a), similar steady states were achieved in both sets of measurements, indicating that steady-state conditions were indeed achieved. Figures 2(b-d) show that the dissociated fraction does not depend on the total [Fe_i] or surface passivation film when plotted against the injection level.

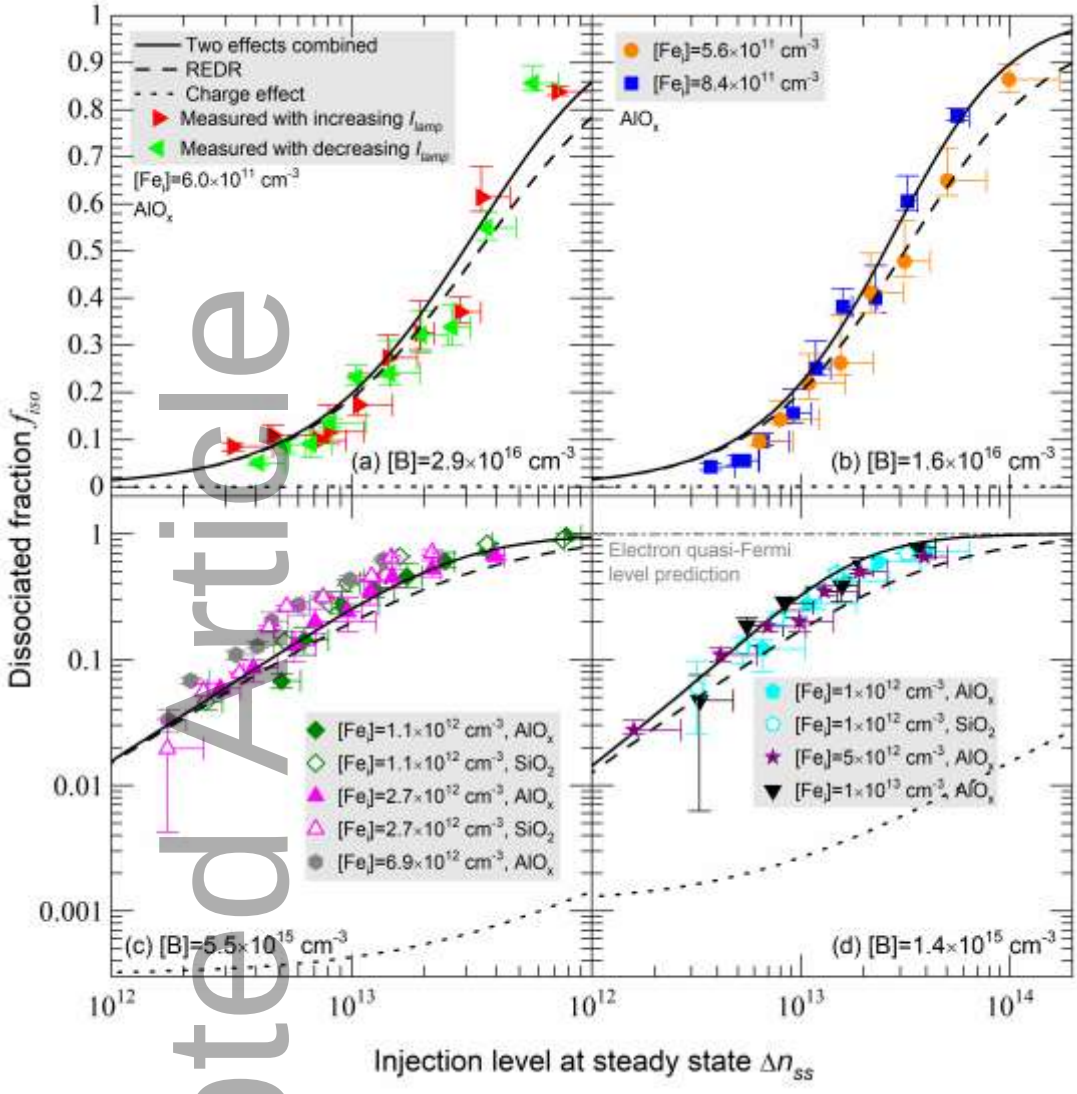

Figure 2. Dissociated fraction f_{iso} as a function of injection level at the steady state Δn_{ss}. Data points were calculated from the lifetime data. $\Delta n_{maxmeasured}$ was used to show the maximum uncertainty in Δn_{ss} (horizontal error bars). The vertical error bars indicate the uncertainty range of f_{iso} calculated over the available injection range. The lines were calculated based on Eq. (7): the predicted dissociated fractions under only the charge effect, and only the REDR effect, and both effects are shown. The results predicted based on the electron quasi-Fermi level approximation are shown in (d).

The injection-dependent charge state of isolated Fe_i was calculated applying the model in Ref.[18]. The defect parameters of Fe_i were taken from Refs.[4,32]. The fraction of [Fe_i^0] to the total isolated Fe_i, f_0 is shown in Figure 3. It can be seen that f_0 increases with the injection for all doping levels. The charge distribution calculated based on the electron quasi-Fermi level approximation is also shown: almost all isolated Fe_i atoms are predicted to be neutrally charged when $\Delta n > 1\times10^8$ cm^{-3} for all the four doping levels. It will be discussed later why this is unreasonable.

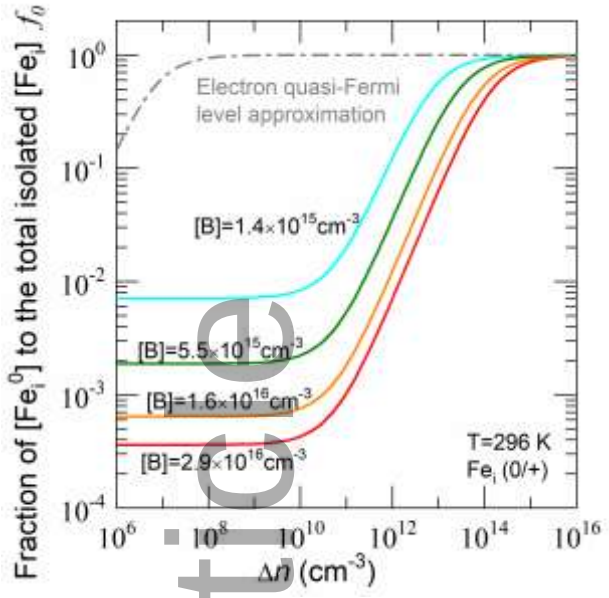

Figure 3. Fraction of Fe_i^0 to the total isolated Fe_i as a function of injection level in p-Si with different doping levels, simulated using the rigorous charge state model (solid lines), and the electron quasi-Fermi level approximation (dash-and-dot line). The electron quasi-Fermi level approximation predicts similar charge distribution of Fe_i for all the four doping levels shown in the figure.

Having determined the fractions of FeB pairs and isolated Fe_i (Figure 2), and the charge distribution of isolated Fe_i (Figure 3), the fraction of every species, FeB, Fe_i^+, and Fe_i^0, in the steady-state system can be calculated. We neglect the changes in $[B^-]$ caused by the pairing, as the doping level $N_A=[B^-]>>[Fe_i]$ in all of the samples. At steady state,[7,8]

$$k_d[\mathrm{FeB}] = k_a N_A[\mathrm{Fe_i^+}]. \quad (4)$$

A ratio k_d/k_a can be calculated based on Eq. (4). k_d and k_a are intrinsic properties of Reaction (1), and are thus independent of the reactants' concentrations. Following the physical mechanisms set out in the REDR theory, the ratios obtained from all the samples are plotted as a function of the recombination rate U on each FeB pair in Figure 4.

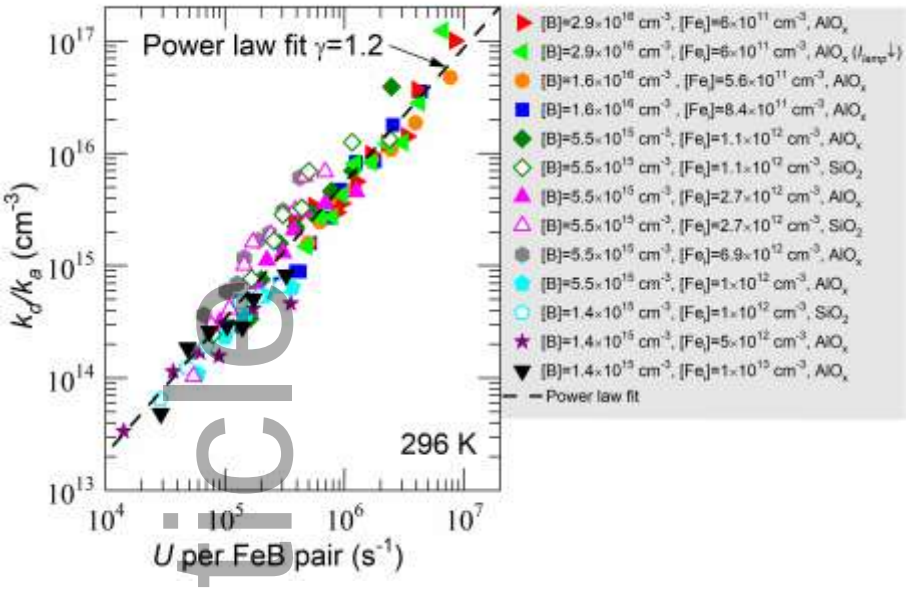

Figure 4. The dissociation/association rate constant ratio k_d/k_a, as a function of the recombination rate U on each FeB pair.

U per FeB pair was calculated based on the SRH statistics. In p-Si:

$$\frac{U}{[\mathrm{FeB}]} = \frac{C_n C_p \Delta n (N_A + \Delta n)}{C_n (n_1 + \Delta n) + C_p (p_1 + N_A + \Delta n)}, \qquad (5)$$

where C_n and C_p are electron and hole capture constants of FeB, respectively. The defect parameters of FeB were taken from Ref.[33]. The parameter U per FeB pair is deemed to be the most suitable independent variable to show the REDR effect. In comparison, the generation rate,[8,14,15] or the injection current density[13] which are more frequently used in the literature, are less ideal for this purpose, because the generated carriers will also recombine through other recombination channels including the unavoidable isolated Fe_i, without contributing to the enhancement of the pair dissociation.

From Figure 4 we can clearly see that the dissociation of FeB under injection *cannot* be purely attributed to charge effects, which do not impact the rate constants k_d and k_a. The thermal-equilibrium value of the rate constant ratio can be calculated via[4,12]

$$\frac{k_d}{k_a} = \frac{N_i}{Z} \exp\left(-\frac{E_b}{k_B T}\right). \qquad (6)$$

where E_b is the equilibrium binding energy of FeB, N_i is the density of interstitial sites in the Si lattice, and Z is the number of possible orientations of the pair around one B atom. At 23 °C, using E_b=0.58 eV,[4,5,7,10] k_d/k_a can be determined to be 1.7×10^{12} cm^{-3}. The much higher k_d/k_a values under injection indicate the REDR effect. In addition, the extracted k_d/k_a ratios are consistent for samples with different doping levels when plotted against U per FeB pair, but were much more scattered when plotted as a function of injection level, generation rate, or U per Fe_i center. This also confirms the REDR mechanism. A power law fit of the data gives a power of 1.2, in reasonable agreement with the theoretical linear relation.[6,20-22] Uncertainties in this result can come from the lifetime measurements, the estimation of injection levels, and defect parameters of isolated Fe_i (in calculating the charge distribution) as well as FeB pairs (in calculating U).

In Ref. [8], k_a was assumed to remain the same as the thermal-equilibrium value, to calculate k_d from the steady-state equation. However, as discussed in Ref.[13], carrier injection not only accelerates the dissociation but may also decelerate the association. Thus, in this study we keep the k_d/k_a ratio as a whole without further separation. It is noteworthy though, that the rate constants k_d and k_a are highly descriptive parameters. The details of the reactions, including the dissociation energy and the binding energy,[4] the short-range and long-range diffusion of isolated Fe_i,[13] are all lumped into the two rate constants. Discussions on these detailed parameters can be found in Refs.[4,13], but further studies, temperature-dependent studies for example, are required to understand their respective dependence on the carrier injection/recombination.

Now we can try to compare the roles of the charge effect and the REDR effect in the dissociation of FeB under injection, based on the results of this investigation. At steady state, the dissociated fraction can be expressed as,

$$f_{iso} = \frac{[Fe_i^+] + [Fe_i^0]}{[Fe_i^+] + [Fe_i^0] + [FeB]} = \frac{1}{1 + N_A \cdot \frac{1 - f_0}{k_d/k_a}}. \qquad (7)$$

In this expression, the charge effect is reflected by the parameter f_0, and the REDR reflected by k_d/k_a. Using the injection-dependent values of f_0 (Figure 3) and k_d/k_a (Figure 4), f_{iso} is plotted in solid lines in Figure 2. The predicted dissociated fraction by the REDR effect was calculated using the injection-dependent k_d/k_a and the thermal-equilibrium f_0, and is shown in dashed lines; and that by the charge effect was using the injection-dependent f_0 and the thermal-equilibrium k_d/k_a, shown in dotted lines. We can see that the REDR effect is much stronger than the charge effect over most of the injection range shown in Figure 2. The dissociated fraction under only the REDR effect is actually very close to that of the two effects combined. This may explain why in some of the previous studies, a linear relation in the REDR effect was still observed even when no charge effect was accounted for.[13] It also means that even if the charge state of Fe_i did not change from positive to neutral, FeB pairs would still be dissociated at a similar rate, as long as a reasonable recombination rate is provided. This highlights the dominant role of REDR effect in dissociating the pairs. In addition, the predicted dissociated fraction under the charge effect based on the electron quasi-Fermi level approximation is shown in Figure 2 (d). Almost all the pairs are predicted to be dissociated from an injection level as low as 10^{11} cm^{-3}, which is obviously not reasonable.

In conclusion, the effects of the charge state of isolated Fe_i and the REDR on the dissociation of FeB pairs in p-Si under injection were investigated and compared in this study. The dynamics of the dissociation/association reactions under different illumination intensities were determined through lifetime measurements and were analyzed as a pathway to access the enhanced reaction rates under the two effects. The charge state of isolated Fe_i was calculated based on a previously proposed charge prediction model. Combining the experimental and modelling results, the dissociation/association rate constant ratio was extracted as a function of the recombination rate on each pair. The extracted ratios were much higher than the thermal value and showed an approximately linear dependence on the recombination rate on each pair, indicating the REDR

effect. The results allowed the charge effect and the REDR effect to be directly compared. The comparison showed that the REDR effect is the dominant effect in most cases.

Acknowledgements

This work was supported by the Australian Renewable Energy Agency (ARENA) through projects RND 005 and 1-A060. C. Sun, Y. Zhu and M. Juhl are supported by the Australian Centre for Advanced Photovoltaics (ACAP) Postdoctoral Research Fellowship. Tim Niewelt of Fh-ISE and Hang Cheong Sio of ANU are gratefully acknowledged for enlightening discussions. The authors would also like to thank Sachin Surve at ANU for the help with sample preparations.

References

1 K. Graff, *Metal impurities in silicon-device fabrication* (Springer Berlin, 2000).
2 E. R. Weber, Applied Physics A **30,** 1-22 (1983).
3 K. Graff and H. Pieper, Journal of the Electrochemical Society **128,** 669-674 (1981).
4 A. Istratov, H. Hieslmair, and E. Weber, Applied Physics A **69,** 13-44 (1999).
5 W. Wijaranakula, Journal of the Electrochemical Society **140,** 275-281 (1993).
6 J. D. Weeks, J. C. Tully, and L. Kimerling, Physical Review B **12,** 3286 (1975).
7 H. Nakashima, T. Isobe, Y. Yamamoto, and K. Hashimoto, Japanese journal of applied physics **27,** 1542 (1988).
8 C. Möller, T. Bartel, F. Gibaja, and K. Lauer, Journal of Applied Physics **116,** 024503 (2014).
9 D. Macdonald, T. Roth, P. N. Deenapanray, K. Bothe, P. Pohl, and J. Schmidt, Journal of Applied Physics **98,** 083509 (2005).
10 H. Lemke, physica status solidi (a) **64,** 215-224 (1981).
11 K. Lauer, C. Möller, D. Debbih, M. Auge, and D. Schulze, in *Determination of activation energy of the iron acceptor pair association and dissociation reaction*, 2016 (Trans Tech Publ), p. 230-235.
12 L. Kimerling, J. Benton, and J. Rubin, Defects and radiation effects in semiconductors 1980**,** 217-222 (1981).
13 L. Kimerling and J. Benton, Physica B+ C **116,** 297-300 (1983).
14 N. Khelifati, H. S. Laine, V. Vähänissi, H. Savin, F. Z. Bouamama, and D. Bouhafs, physica status solidi (a) **216,** 1900253 (2019).
15 L. Geerligs and D. Macdonald, Applied Physics Letters **85,** 5227-5229 (2004).
16 T. Bartel, F. Gibaja, O. Graf, D. Gross, M. Kaes, M. Heuer, F. Kirscht, C. Möller, and K. Lauer, Applied Physics Letters **103,** 202109 (2013).
17 H. Reiss, C. Fuller, and F. Morin, Bell Labs Technical Journal **35,** 535-636 (1956).
18 C. Sun, F. E. Rougieux, and D. Macdonald, Journal of Applied Physics **117,** 045702 (2015).
19 H. Conzelmann, K. Graff, and E. Weber, Applied Physics A **30,** 169-175 (1983).
20 D. Lang, Annual review of materials science **12,** 377-398 (1982).
21 L. Kimerling, Solid-State Electronics **21,** 1391-1401 (1978).
22 T. Markvart, Solar Cells **2,** 49-53 (1980).
23 D. Macdonald, L. Geerligs, and A. Azzizi, Journal of Applied Physics **95,** 1021-1028 (2004).
24 R. A. Sinton and A. Cuevas, Applied Physics Letters **69,** 2510-2512 (1996).
25 See https://www.btimaging.com/products-c1g2d for the information of the LIS-R1 PL imaging system from BT Imaging, Nov-2020.
26 A. Herguth, Energy Procedia **124,** 53-59 (2017).
27 A. Liu and D. Macdonald, physica status solidi (RRL)–Rapid Research Letters **12,** 1700430 (2018).
28 F. Kersten, P. Engelhart, H.-C. Ploigt, A. Stekolnikov, T. Lindner, F. Stenzel, M. Bartzsch, A. Szpeth, K. Petter, and J. Heitmann, in *A new mc-Si degradation effect called LeTID*, 2015 (IEEE), p. 1-5.
29 T. Niewelt, F. Schindler, W. Kwapil, R. Eberle, J. Schön, and M. C. Schubert, Progress in Photovoltaics: Research and Applications **26,** 533-542 (2018).
30 C. E. Chan, D. N. Payne, B. J. Hallam, M. D. Abbott, T. H. Fung, A. M. Wenham, B. S. Tjahjono, and S. R. Wenham, IEEE Journal of Photovoltaics **6,** 1473-1479 (2016).

[31] D. Macdonald, T. Roth, P. Deenapanray, T. Trupke, and R. Bardos, Applied Physics Letters **89,** 142107 (2006).
[32] D. Macdonald, J. Tan, and T. Trupke, Journal of Applied Physics **103,** 073710 (2008).
[33] D. Macdonald, A. Cuevas, and J. Wong-Leung, Journal of Applied Physics **89,** 7932-7939 (2001).

GA: The dissociation of FeB pairs in p-type silicon under injection is often explained by the charge state change of Fe_i, but is also sometimes interpreted as a Recombination-Enhanced Defect Reaction (REDR) mechanism. The experiments designed in this study allow the two effects to be more distinctly separated and directly compared. The results highlight the dominant role of the REDR effect.